Available online at www.sciencedirect.com
ScienceDirect
Journal of Nuclear Materials 360 (2007) 177–185
journal of nuclear materials
www.elsevier.com/locate/jnucmat

Role of microstructure and heat treatments on the desorption kinetics of tritium from austenitic stainless steels

J. Chêne [a,*], A.-M. Brass [a], P. Trabuc [b], O. Gastaldi [b]

[a] *Laboratoire de Physico-Chimie de l'Etat Solide, CNRS, UMR 8648, Université Paris-Sud, 91405 Orsay cedex, France*
[b] *Association EURATOM-CEA Cadarache, DTN/STPA/LPC, 13108 Saint Paul Lez Durance, France*

Received 4 April 2006

Abstract

The liquid scintillation counting of solid samples (LSC-SS technique) was successfully used to study the role of microstructure and heat treatments on the behavior of residual tritium in several austenitic stainless steels (as-cast remelted tritiated waste, 316LN and 321 steels). The role of desorption annealing in the 100–600 °C range on the residual amount of tritium in tritiated waste was investigated. The residual tritium concentration computed from surface activity measurements is in good agreement with experimental values measured by liquid scintillation counting after full dissolution of the samples. The kinetics of tritium desorption recorded with the LSC-SS technique shows a significant desorption of residual tritium at room temperature, a strong barrier effect of thermal oxide films on the tritium desorption and a dependance of the tritium release on the steels microstructure. Annealing in the 300–600 °C range allows to desorb a large fraction of the residual tritium. However a significant trapping of tritium is evidenced. The influence of trapping phenomena on the concentration of residual tritium and on its dependance with the annealing temperature was investigated with different recrystallized and sensitized microstructures. Trapping is evidenced mainly below 150 °C and concerns a small fraction of the total amount of tritium introduced in austenitic steels. It presumably occurs preferentially on precipitates such as Ti(CN) or on intermetallic phases.

1. Introduction

In the nuclear industry, several scientific and technical challenges are related with the interaction of hydrogen and its isotopes (deuterium, tritium) with microstructural defects in structural materials. Among others, several key issues can be mentioned:

– the prediction and prevention of the role of hydrogen in the environmental degradation (hydrogen embrittlement: H.E., stress corrosion cracking: SCC,...) of structural materials, which remains a priority in various nuclear activities [1–3],
– the management of tritiated waste which requires a precise control of very low tritium concentration in the materials (i.e.: 0.1 Ci/ton

* Corresponding author. Present address: Laboratoire d'Etude de la Corrosion Aqueuse, DEN/DANS/DPC/SCCME, CEA Saclay Bât. 458, F91191 Gif sur Yvette, France. Tel.: +33 01 69 08 59 29; fax: +33 01 69 08 15 86.
E-mail address: jacques.chene@cea.fr (J. Chêne).

0022-3115/$ - see front matter © 2006 Elsevier B.V. All rights reserved.
doi:10.1016/j.jnucmat.2006.10.010

corresponds to a tritium concentration as low as 10^{-5} ppm wt) [4,5],
– the tritium handling and tritium inventory in fusion technology which needs precise data on the tritium interactions (diffusion, trapping,....) with various alloys including structural materials [6,7].

For these reasons one needs to improve the knowledge of the interactions of tritium with the microstructure (microstructural defects, irradiation-induced defects,...) of various materials including iron and nickel base alloys. This also requires an improvement of non destructive techniques used for the measurement of both the concentration and the desorption of residual tritium.

In this paper we present the results of a first set of experiments aimed at characterizing the role of microstructural defects (especially carbides and carbonitrides) and of desorption heat treatments, on the desorption kinetics and residual concentration of tritium in austenitic stainless steels. For this purpose a new procedure was used to allow the non destructive study of massive tritiated metallic samples with the liquid scintillation counting technique.

2. Experimental

2.1. Material

Two types of austenitic stainless steels were used in this study.

An austenitic alloy (alloy W), representative of a tritiated waste, was obtained from the remelting under vacuum of tritiated austenitic stainless steels. Significant local variations have been observed in the composition of the ingot obtained from remelted wastes. However the average composition (wt%) of this austenitic steel is the following: Cr 18, Ni 12, Fe 67, various amounts of Mo, Mn, Si, Nb, Ti. The microstructure of this as-cast austenitic alloy is illustrated in Fig. 1. It exhibits large dendritic grains and the presence of numerous precipitates or secondary phases (manganese sulphide, chromium carbides, δ ferrite, intermetallics,...). Small coupons were taken in different parts of the ingot. Depending on the location in the ingot, the residual concentration of tritium ranged from 70 kBq/g (batch 1) to 114 ± 21 kBq/g (batch 2). These values were measured, by liquid scintillation after dissolving the specimen in acid solutions. Some of these coupons were aged at different temperatures for different times under an argon flow in order to favor the tritium desorption.

Some other samples were taken from as received plates of 316LN and 321 austenitic steels. The chemistry of these alloys is reported in Table 1. The samples were given different heat treatments reported in Table 2 in order to obtain four typical microstructures with different types of precipitates [8,9]. As shown in Fig. 2(a) and (b), a very limited precipitation of carbides ($M_{23}CN_6$) or nitrides (Cr_2N) is observed in the so-called 'recrystallized' microstructure of alloy 316LN whereas a strong intragranular and intergranular precipitation occurs in the 'sensitized' alloy. The recrystallized microstructure of the 321 steel (Fig. 2(c)) shows the presence of intragranular titanium nitrides and of small intergranular precipitates (presumably chromium carbides partially substituted by titanium). The presence of very small coherent titanium carbides is also expected.

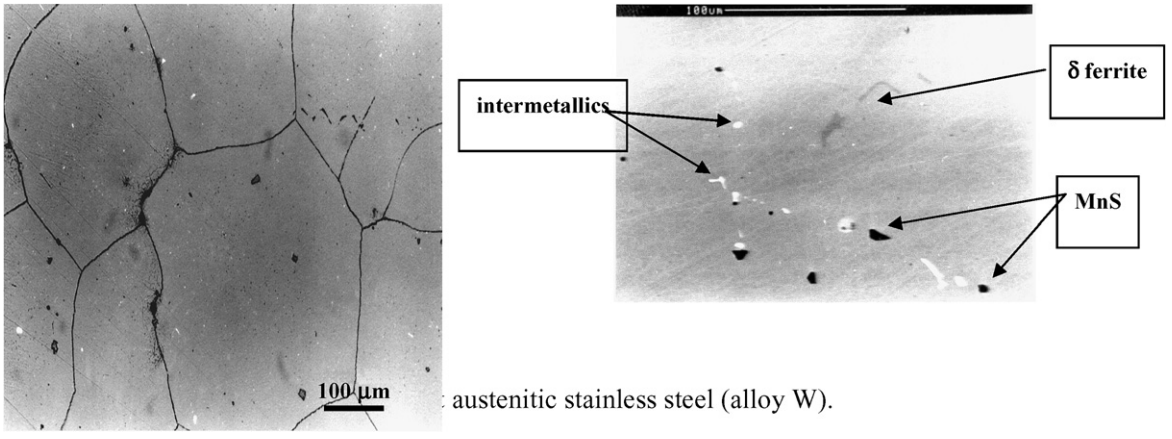

Fig. 1. Microstructure of the as-cast austenitic stainless steel (alloy W).

Table 1
Chemistry of the austenitic steels (% wt)

Alloy	Cr	Ni	Mo	C	Mn	Si	Ti	N	S	P	Cu	Co
316LN	17.4	13.4	2.50	0.029	1.62	0.50	–	**0.15**	0.002	0.029	0.075	0.02
321	17.2	9.2	0.53	**0.054**	1.57	0.50	**0.375**	0.02	0.0002	0.031	–	–

Table 2
Selected heat treatments

Alloy/heat treatment	Recrystallized	Sensitized
316LN	1 h, 1090 °C (+W.Q.)	Recryst. + 700 °C, 5 h after 30% cold worked
321	1 h, 1200°C (+W.Q.)	Recryst. + 800 °C, 5 h

The sensitization treatment of 321 steel favors a strong intragranular precipitation of very small particules identified as carbides or carbonitrides.

2.2. Techniques

2.2.1. Hydrogen and tritium charging and desorption

In order to study the microstructural dependance of tritium absorption and desorption in 316LN and 321 steels, tritium was introduced in small coupons ($10 \times 10 \times 0.3\ mm^3$) by cathodic charging in molten salts. This cathodic charging technique, described elsewhere [10], was also used in order to introduce hydrogen instead of tritium in some specimens. The cathodic charging conditions are reported in Table 3.

2.2.2. Desorption heat treatments

Some hydrogenated or tritiated coupons of alloys W, 316LN and 321 were given an aging treatment for various temperature/time conditions in order to desorb the fraction of diffusible tritium available at the considered aging temperature. The different conditions used for desorption are reported in Table 3.

2.2.3. Hydrogen concentration measurement

The total hydrogen concentration remaining in the samples after cathodic charging and annealing was measured by melting the hydrogen-charged

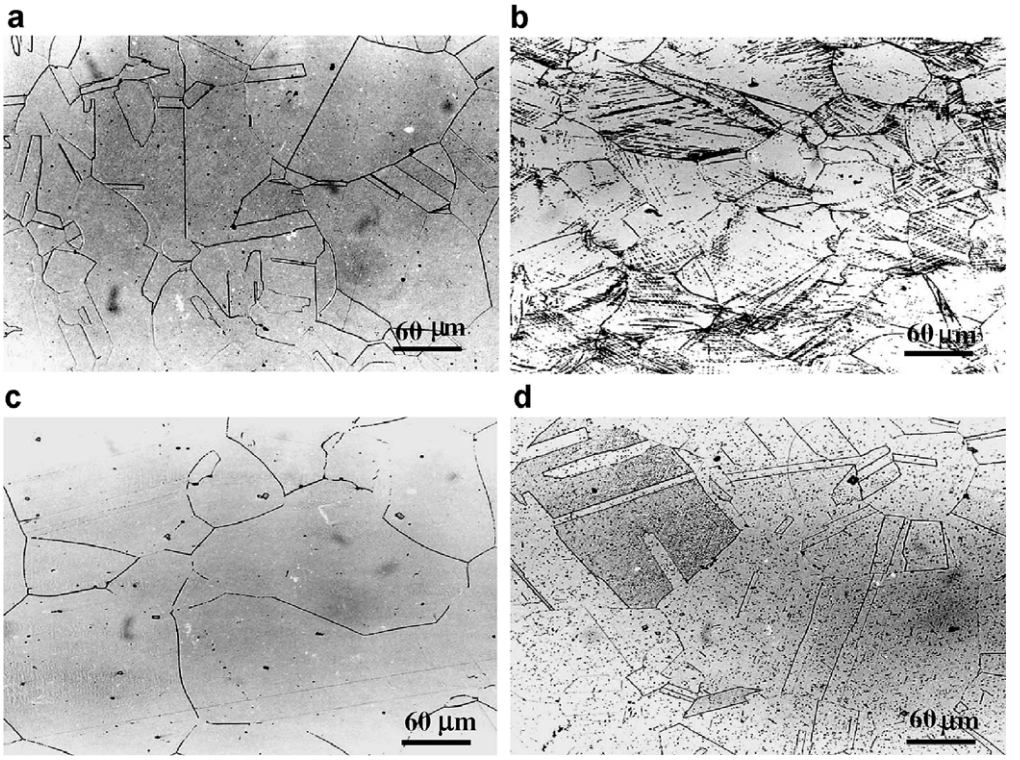

Fig. 2. Typical microstructures of 316 LN and 321 austenitic stainless steels: (a) 316LN recrystallized (1 h, 1090 °C, + W.Q.), (b) 316 LN sensitized (rec. + 30% c.w. + 5 h, 700 °C), (c) 321 recrystallized (1 h, 1090 °C, + W.Q.) and (d) 321 sensitized (rec. + 5 h, 800 °C).

Table 3
Selected conditions for the cathodic charging and for the desorption of hydrogen or tritium

Cathodic charging in molten salts	Desorption annealing after H or ^{3}H charging (dry Ar flow)
Hydrogen: 300 °C, 1 h, 500 mA cm^{-2}	100 °C, 528 h 150 °C, 70 h
Tritium: 150 °C, 3 h, −1000 mV$_{Ag/Ag+}$	200 °C, 14 h
Specific activity: 4.7×10^7 Bq g^{-1}	600 °C, 20 h + 600 °C, 4 h + 600 °C, 4 h[a]

[a] This desorption annealing was given to alloy W prior to cathodic charging in molten salts for a full desorption of the residual tritium already present in the waste.

samples at 1500 °C with the nitrogen-carrier-fusion thermal conductivity method (JUWE H-Mat 2500 analyzer).

2.2.4. Measurements of the tritium activity on the surface and of the tritium desorption rate

The liquid scintillation counting of solid samples (LSC-SS technique) was used for the non destructive monitoring of the tritium behavior in massive tritiated samples before and after desorption heat treatment [5,11,12]. The capabilities of the technique are sketched in Fig. 3. For a tritiated specimen in contact with the scintillation cocktail, and in the absence of a significant desorption of tritium (short counting times, low tritium diffusivity), the collected β emission comes from a thin superficial layer. The thickness ($R_m \approx 1$ μm) of this analyzed layer is a function of the absorption distance in the solid of the low energy beta radiations of tritium. In such conditions, the technique allows to measure the tritium activity on the near surface of the specimen and, assuming an homogeneous distribution of tritium in the sample, a value of the tritium concentration can be assessed from the value of the surface activity. If tritium atoms desorb from the sample during the counting period they are readily transferred in the scintillation cocktail leading to a gradual increase of the β emission from the volume of scintillation cocktail stored in the vial with the specimen. The recording, at room temperature, of the dependance with time of the cumulated amount of tritium in the vial gives the tritium desorption rate from the specimen.

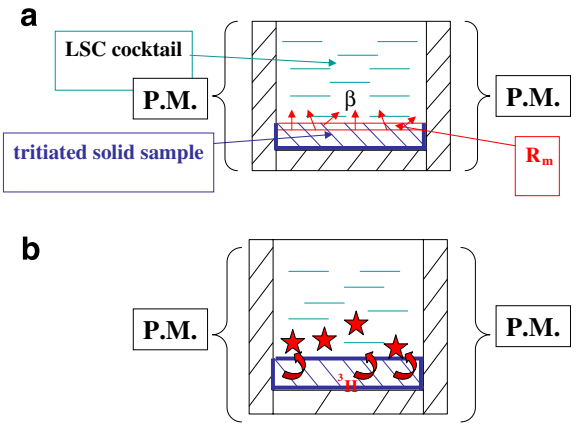

Fig. 3. Schematic view of the liquid scintillation counting of massive tritiated specimens (LSC-SS technique): (a) without tritium desorption from the solid sample and (b) tritium transfer from the solid to the LSC cocktail.

Finally, the LSC-SS technique can be used for high sensitivity measurements of both the surface activity representative of the residual concentration of tritium and of the tritium desorption rate. Moreover several measurements can be made on a same specimen exposed to successive desorption heat treatments performed at growing temperatures.

In order to get reproducible results a careful preparation of the sample surface is required. In these experiments a repolishing of the surface up to paper 4000 grade was followed by successive cleaning in distilled water and ethanol. Moreover the area of the samples surface in contact with the scintillator has been well delimited.

3. Results

3.1. Role of a desorption annealing on the residual amount of tritium in tritiated stainless steel waste

Small coupons ($10 \times 7 \times 1$ mm^3) of the remelted austenitic steel (alloy W) were used for this study.

3.1.1. Surface activity and tritium release at 20 °C before annealing

The tritium activity on the surface and an hypothetic desorption at room temperature of the residual tritium were measured with the LSC-SS technique on several samples to test the reproducibility of the measurements. The raise of the tritium activity in the vial plotted as a function of time (Fig. 4(a)) demonstrates a significant desorption of residual tritium from each specimen at room temperature. The reproducibility of the results is fairly good both for the surface activity (mean activity

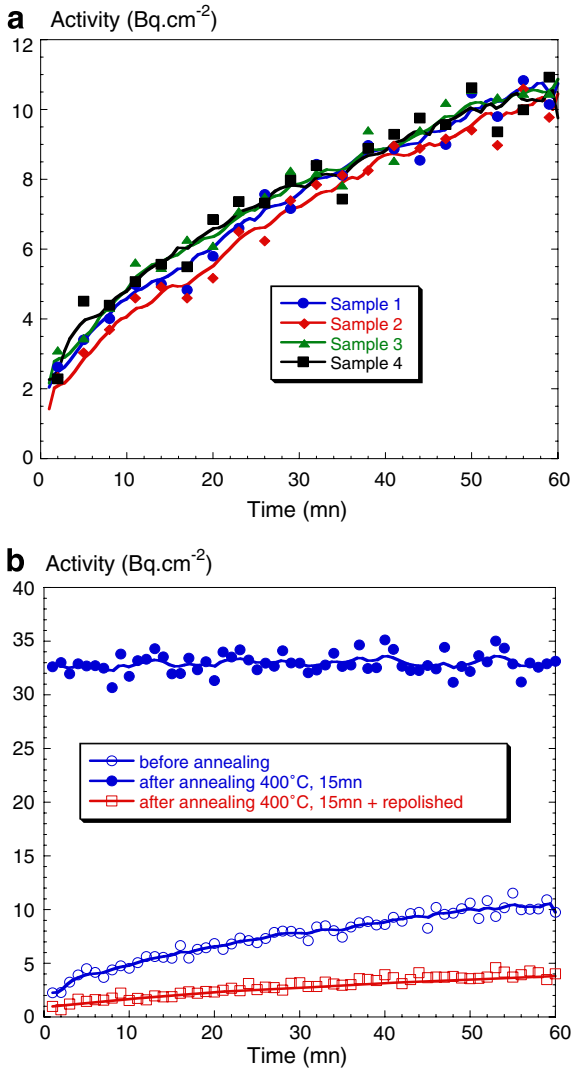

Fig. 4. Tritium desorption profiles recorded at 20 °C from massive samples (alloy W, batch 1): (a) profile obtained on four specimens of the same batch and (b) profiles obtained on the same sample successively: before desorption annealing, after annealing (15 mn, 400 °C) and after removing the oxide layer (repolishing).

at $0 < t < 3$ mn) and for the rate of tritium release. The mean value of the surface activity measured with ten samples (batch 2) is 5.5 ± 1.2 Bq cm^{-2} and, for a counting time of 60 mn, the mean desorption rate is $1 \times 10^{-3} \pm 0.3 \times 10^{-3}$ Bq cm^{-2} s^{-1}.

3.1.2. Surface activity and tritium release at 20 °C after annealing

A very thin oxide layer (a few tens of nm) is grown on the samples surface during annealing in the 100–600 °C. As illustrated in Fig. 4(b) the presence of this oxide film is associated with a very strong increase of the surface activity: about two orders of magnitude for annealing in the temperature range 300–500 °C. This indicates a strong tritium enrichment of the superficial oxide film which results from the formation of a tritiated hydroxide on the surface. Moreover the stationary value recorded for the tritium activity in the vial when the sample is oxidised, indicates the absence of tritium release at 20 °C from the specimen. This barrier effect of the oxide film is clearly illustrated in Fig. 4(b) since after removing of the oxide film (repolishing of the surface of the specimen) a significant desorption of the residual tritium is observed again. However when compared to the as received state, the drop of both the surface activity and the tritium release results from the partial tritium desorption occurring during the short annealing (15 mn) at 400 °C.

3.1.3. Role of the temperature of the desorption annealing on the residual tritium concentration

In order to assess the role of the annealing temperature on the desorption of the residual tritium, several specimens were given a desorption annealing for the same time (20 h) but different temperatures ranging from 100 to 600 °C. A plot of the surface activity (measured after removing the oxide film) and of the mean desorption rate of residual tritium (computed over 1000 mn at 20 °C) is reported in Fig. 5(a) as a function of the annealing temperature. It shows a steep decrease of these values in the 100–300 °C temperature range.

The residual concentration of tritium in annealed samples was measured by liquid scintillation after full dissolution in acid solutions. These values are plotted as a function of the annealing temperature in Fig. 5(b). A strong drop of the residual concentration is observed in the 100–300 °C in agreement with the results reported in Fig. 5(a). However the significant residual concentration measured for the samples annealed above 300 °C suggests the existence of trapping phenomena.

3.2. Role of the microstructure of austenitic stainless steels on the absorption/desorption of hydrogen or tritium

A systematic investigation of the influence of trapping phenomena (especially trapping on precipitates associated with sensitization heat treatments) on the concentration of residual tritium and on its dependence with the annealing temperature was

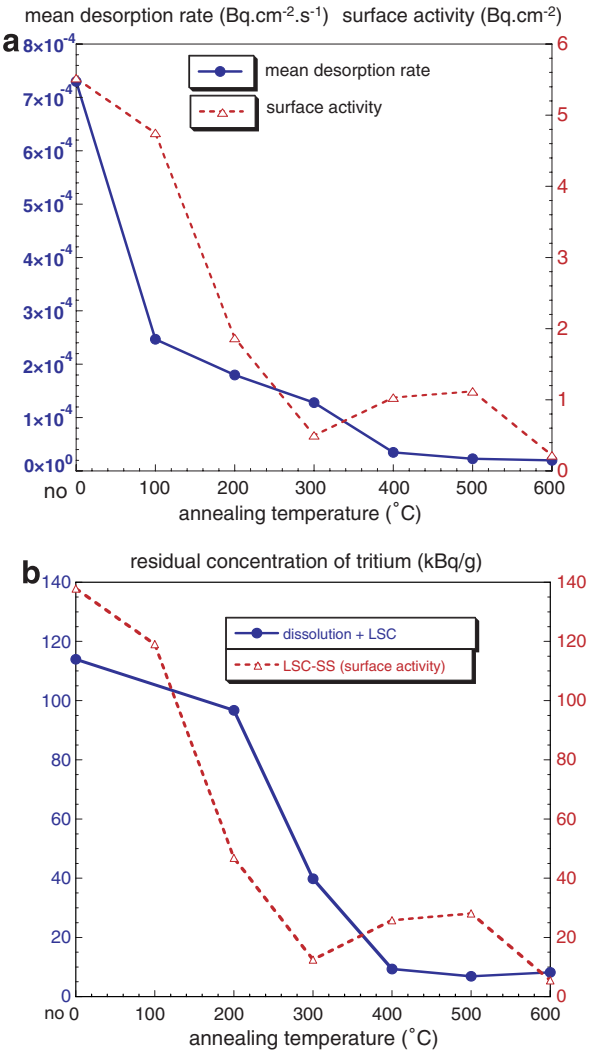

Fig. 5. Role of the annealing temperature on the amount of residual tritium in a tritiated stainless steel waste (alloy W, batch 2, annealing time: 20 h): (a) role of the annealing temperature on the surface activity and the mean desorption rate (counting time 1000 mn) and (b) role of the annealing temperature on the residual concentration of tritium measured by liquid scintillation counting after dissolution or computed with the experimental data of surface activity.

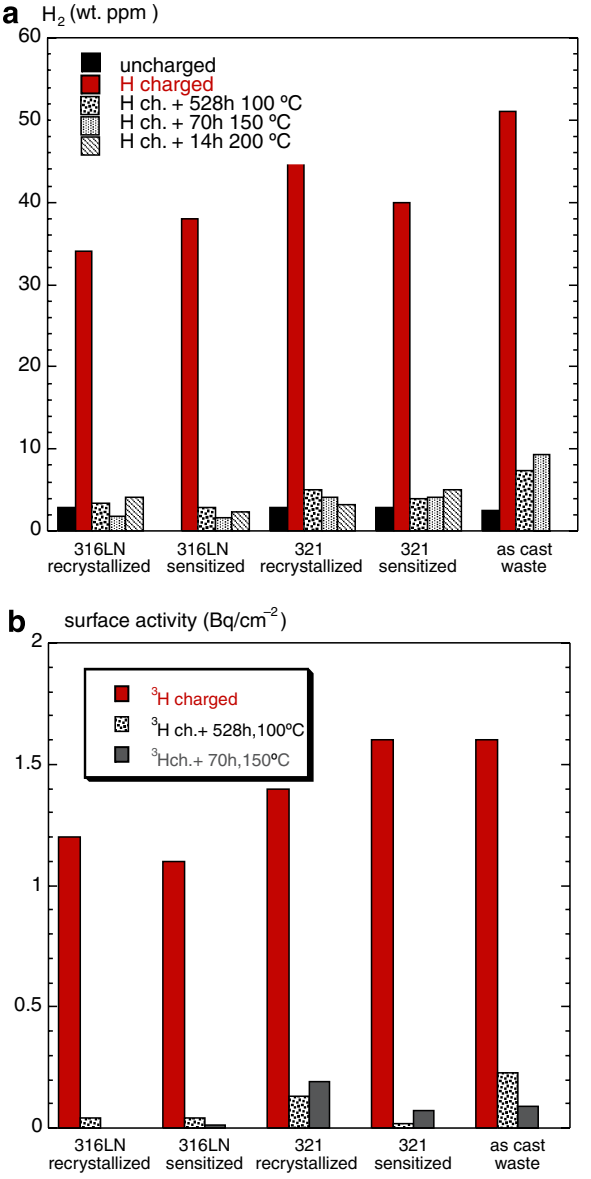

Fig. 6. Role of the microstructure of austenitic stainless steels on the absorption/desorption of hydrogen or tritium: (a) residual concentration of hydrogen measured by extraction at high temperature after a cathodic charging followed by a desorption annealing and (b) surface activity measured on tritiated samples after a cathodic charging followed by a desorption annealing.

performed with the as-cast alloy W and the four model microstructures described in Section 2.1 and Fig. 2.

3.2.1. Role of the microstructure on the hydrogen concentration

In order to get a better insight on the role of the microstructure on hydrogen trapping several specimens of each microstructure were first cathodically charged for 1 h at 300 °C (Table 3). Some samples were then given a desorption annealing (Table 3) and the residual concentration of hydrogen was measured by extraction at high temperature. The hydrogen concentration analysis was performed with the nitrogen carrier fusion thermal conductivity method after cathodic charging of the different microstructures; the results are summarized in Fig. 6(a). The hydrogen concentration in uncharged

specimens is about 3 ppm wt whatever the microstructure. For the cathodic charging conditions used (300 °C, 1 h, $d = 500$ mA cm^{-2}) the hydrogen concentration introduced in the specimens ranges between 35 and 50 ppm wt with a maximum concentration measured in the as-cast microstructure of alloy W. However the possible effect of the microstructure on H absorption is not clearly evidenced for these charging conditions. Some discrepancies are observed for the residual amount of hydrogen after desorption at 100, 150 and 200 °C. Moreover, taking into account the concentration of H already present in the uncharged specimens, the residual concentration after desorption annealing is very low especially in the 316LN microstructures. When compared to the total amount of hydrogen introduced by cathodic charging, the fraction of hydrogen trapped in these microstructures is small. A possible dependence of the concentration of diffusible hydrogen on changes in the lattice parameter of the alloys, was not investigated.

3.2.2. Role of the microstructure on the tritium absorption and desorption

The surface activity of tritiated specimens was measured with the LSC-SS technique, in order to characterize the absorption and desorption of tritium in the different microstructures. The results are reported in Fig. 6(b). As the uncharged samples are free of tritium the results clearly show the existence of a significant trapping of tritium up to 150 °C in all of the microstructures except the almost precipitate free recrystallized 316LN. The surface activities measured after annealing indicate that the extent of trapping is more pronounced for the recrystallized microstructure of 321 steel and for the as-cast alloy W.

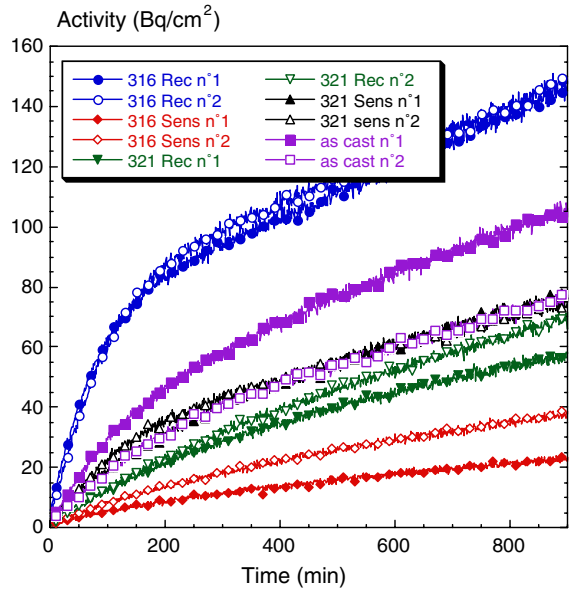

Fig. 7. Role of the microstructure on the cumulated amount of tritium released at 20 °C from austenitic stainless steels.

The rate of tritium desorption at 20 °C and its dependance with the microstructure of the alloys was also recorded with the LSC-SS technique. The results reported in Fig. 7 show a strong effect of the microstructure on the amount of tritium released at 20 °C. As shown in Fig. 6 this effect cannot be related with marked changes in the concentration of tritium on the surface or in the bulk.

4. Discussion

4.1. Surface activity and tritium concentration

Assuming an homogeneous distribution of tritium in the samples, an estimate of the tritium concentration can be computed from the experimental value of the surface activity according to a simplified procedure reported elsewhere [13]. With $R_m = 0.7$ μm for the absorption distance of the 18 keV β radiation of ^{3}H in austenitic stainless steel a value of 140 ± 30 kBq g^{-1} is computed for the tritium concentration associated with a surface activity of 5.5 ± 1.2 Bq cm^{-2} (cf. Section 3.1). This value fairly agrees with the experimental value of 114 ± 21 kBq g^{-1} obtained by liquid scintillation counting after full dissolution of the samples (cf. Section 2.1). The same procedure was used to evaluate the dependance of the residual concentration of tritium with the annealing temperature. The computed concentration values are reported in Fig. 5(b) and compared with the experimental data obtained after dissolution of the samples. In spite of some discrepancies, the dependance with the annealing temperature of the computed values and of the experimental values exhibit a good correlation. The strong drop of the residual concentration in the 100–300 °C temperature range is to be compared with the computed concentration profiles of residual tritium reported in Fig. 8(a). These profiles were obtained for 0.1 cm thick samples assuming a bulk diffusion control of ^{3}H desorption from a plane sheet. The value of the diffusion coefficient of ^{3}H was obtained for each temperature from the Arrhenius law reported by Tison for H diffusivity in a

316L steel [14]. In the 100–300 °C range, the comparison of the computed concentration profiles (Fig. 8(a)) with the residual concentration (Fig. 5(b)) indicates that an important fraction of the residual tritium present in alloy W desorbs at moderate temperatures and that the desorption is controlled by the diffusion of ^3H in the lattice. However, the concentration profile after 20 h annealing at 300 °C shows that the diffusible ^3H almost completely desorbs at this temperature whereas a significant residual concentration is measured after annealing above 300 °C. This can be explained by trapping phenomena on microstructural defects and secondary phases present in alloy W.

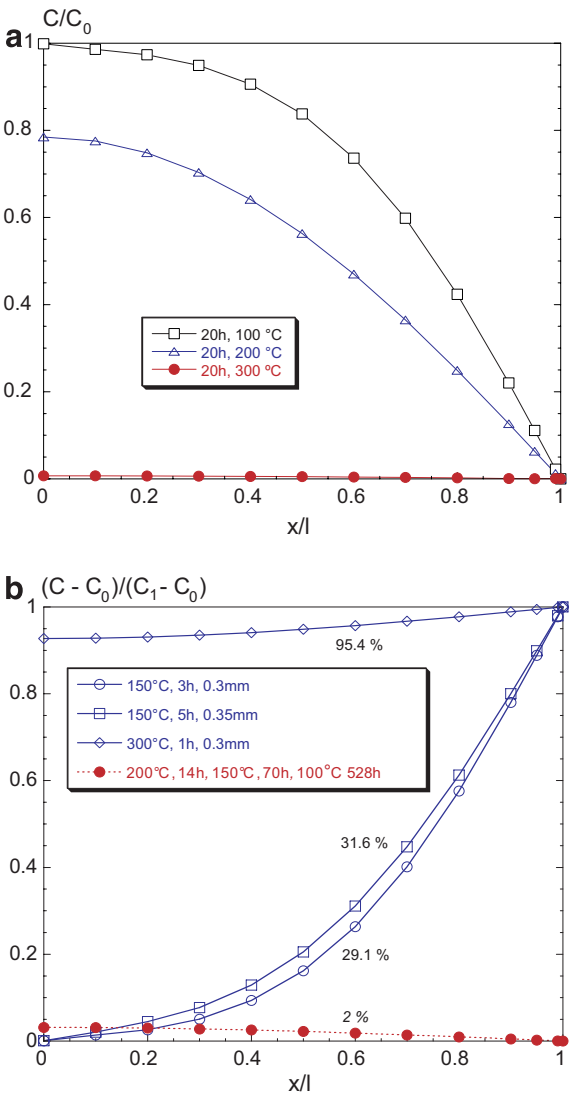

Fig. 8. Computed normalized concentration profiles of hydrogen in the half thickness of a sheet of austenitic stainless steel after different conditions of cathodic charging or desorption: (a) residual concentration of H in 0.1 cm thick samples after desorption annealing for 20 h at 100, 200 or 300 °C and (b) concentration profiles of H in 0.03 cm thick samples after cathodic charging for 3 h at 150 °C or 1 h at 300 °C or after desorption for 528 h at 100 °C, 70 h at 150 °C or 14 h at 200 °C.

4.2. Hydrogen and tritium trapping in austenitic stainless steels

Neglecting the isotopic effect, the H concentration profiles associated with the conditions of cathodic charging and of desorption reported in Table 3 are plotted in Fig. 8(b). These profiles show an almost homogeneous distribution of H in the samples after 1 h cathodic charging at 300 °C (95% of the volume of the specimen is hydrogenated). In such a way the hydrogen concentration values do not depend on the specimens geometry. Assuming H diffusivity at 300 °C independent of the microstructure, the total amount of H in the samples would mainly depend on H solubility in the austenitic stainless steels for the considered charging conditions and on a possible H trapping on defects and secondary phases. Desorption annealing at 100, 150 and 200 °C were performed with selected times in order to ensure an almost complete desorption of the diffusible hydrogen at the considered temperature (2% of residual H, cf. Fig. 8(b)). After annealing in the 100–200 °C range the residual concentrations of hydrogen in the cathodically charged samples of 321 steel and as-cast alloy W are significantly larger than in the uncharged samples (Fig. 6(a)). This indicates the existence of H trapping in these microstructures up to 200 °C. On the opposite, after cathodic charging, the retention of H in annealed 316LN samples is of the same order of magnitude as uncharged samples (Fig. 6(a)). This suggests a low retention of cathodic H in this alloy for these annealing conditions. However except in the case of the as-cast alloy, the fraction of trapped hydrogen is small (about 5%) when compared to the total amount of H introduced in the samples. Moreover the uncertainties on the hydrogen concentration data obtained with the high temperature extraction technique do not allow to relate H trapping with the nature and density of precipitates.

The surface activity of the tritiated samples measured with the LSC-SS technique reflects the role of each microstructure on the concentration of residual ^3H, in agreement with hydrogen concentration measurements. Significant amounts of tritium remain trapped in 321 steel and in as cast alloy W

after annealing at 150 °C. Moreover the high sensitivity of the technique shows the presence of a small fraction of ^{3}H trapped in 316LN steel. With this more sensitive technique a value of about 10% is obtained for the fraction of ^{3}H trapped in the microstructure of 321 and as-cast alloy W. Whereas autoradiographic observations of the tritium distribution in the microstructure are required in order to precise the role of precipitates (nature, density, coherency, ...) on ^{3}H trapping, the relatively large fraction of residual tritium in the recrystallized 321 steel after desorption at 150 °C (Fig. 6(b)) is presumably a consequence of ^{3}H trapping on coherent titanium carbides. In the complex as-cast microstructure of alloy W a preferential trapping on manganese sulphide and on Nb rich intermetallic phases has been already observed by tritium autoradiography [15].

Additional studies are required to relate trapping phenomena to the observed effect of microstructure on the rate of tritium release (Fig. 7). However, the strong drop of the tritium desorption rate in the sensitized 316LN alloy is presumably a consequence of the reversible trapping of ^{3}H on the very dense network of carbides or nitrides precipitates uniformly distributed in the microstructure (Fig. 2).

5. Conclusions

The non destructive and very sensitive technique of liquid scintillation counting of solid samples (LSC-SS) is convenient to study the behavior of tritium in metallic materials such as austenitic steels. The surface activity measured with this technique can be used to estimate the tritium concentration in the material and the tritium desorption analysis allows to characterize the role of oxide film or of the alloys microstructure on the kinetics of tritium desorption.

Thin thermal oxide films grown on the surface of austenitic steels act as a barrier to the desorption of residual tritium. However annealing in the 300–600 °C range allows to desorb most of the residual tritium.

The tritium absorption/desorption depends on the steels microstructure. A significant trapping of tritium is shown to occur preferentially in sensitized microstructures on precipitates such as Ti(CN) or on intermetallic phases. However tritium trapping occurs mainly below 150 °C and concerns a small fraction of the total amount of tritium introduced in austenitic steels.

Acknowledgements

The authors like to thank A. Lassoued for his technical assistance in part of this study.

J.P. Daclin (CEA/DAM/DTMN 21120 Is sur Tille) is gratefully acknowledged for providing alloy W.

References

[1] D.M. Symons, J. Nucl. Mater. 265 (1999) 225.
[2] D. Noel, O. de Bouvier, F. Foct, T. Magnin, J.D. Mithieux, F. Vaillant, in: T. Magnin (Ed.), Corrosion-Deformation Interactions, The Institute of Materials Pub., 1997, p. 435.
[3] J. Chêne, A-M. Brass, Metall. Mater. Trans. 35A (2004) 457.
[4] K.Y. Wong, B. Hircq, R.A. Jalbert, W.T. Shmayda, Fusion Eng. Des. 16 (1991) 159.
[5] S. Rosanvallon, G. Marbach, A.-M. Brass, J. Chêne, J.P. Daclin, Fusion Eng. Des. 51&52 (2000) 605.
[6] S. Tanaka, M. Nishikawa, Y. Ichimasa, M. Nishi, Fusion Sci. Technol. 41 (2002) 305.
[7] D. Murdoch, Ch. Day, M. Glugla, R. Laesser, A. Mack, R-D. Penzhorn, A. Busigin, K. Maynard, O. Kveton, Fusion Sci. Technol. 41 (2002) 1018.
[8] D. Peckner, I.M. Bernstein (Eds.), Handbook of Stainless Steels, Mc Graw Hill, New York, 1978 (Chapter 4).
[9] R. Singh, B. Ravikumar, A. Kumar, P.K. Dey, I. Chattoraj, Metall. Mater. Trans. 34A (2003) 2003.
[10] P. Lacombe, M. Aucouturier, J. Chêne, in: R. Gibala, R.F. Hehemann (Eds.), Hydrogen Embrittlement and Stress Corrosion Cracking, TRMS AIME Pub., Warrendale, PA, 1996, p. 79.
[11] J. Chêne, A.-M. Brass, Scripta Mater. 40 (5) (1999) 537.
[12] A. Lassoued, J. Chêne, A.-M. Brass, O. Gastaldi, P. Trabuc, G. Marbach, Fusion Eng. Des. 75–79 (2005) 731.
[13] J. Chêne, P. Trocellier, J. Non Cryst. Solids 337 (2004) 86.
[14] P. Tison, Influence de l'hydrogène sur le comportement des métaux, in: CEA Service de documentation, Saclay, France (Eds.), CEA-R-5240 (1), ISSN 0429-3460, 1984, p. 1.
[15] A. Lassoued, A.-M. Brass, J. Chêne, Gestion des aciers tritiés, Rapport contrat CEA-CNRS-UPS no. B5358, December 2003.